Final Draft

of the original manuscript:

Chalupsky, J.; Hajkova, V.; Altapova, V.; Burian, T.; Gleeson, A.J.; Juha, L.; Jurek, M.; Sinn, H.Stoermer, M.; Sobierajski, R.; Tiedtke, K.; Toleikis, S.; Tschentscher, T.; Vysin, L.; Wabnitz, H.; Gaudin, J.

Damage of amorphous carbon induced by soft x-ray femtosecond pulses above and below the critical angle

In: Applied Physics Letters (2009) AIP

DOI: 10.1063/1.3184785

Damage of amorphous carbon induced by soft x-ray femtosecond pulses above and below the critical angle

J. Chalupský, V. Hájková, L. Vyšín, T. Burian, L. Juha

Institute of Physics, Academy of Sciences of the Czech Republic, Na Slovance 2, 182 21 Prague 8, Czech Republic

J. Gaudin, V. Altapova, H. Sinn, Th. Tschentscher

European XFEL, c/o DESY Notkestr. 85 D-22607 Hamburg, Germany

M. Jurek, R. Sobierajski

Institute of Physics, Polish Academy of Sciences, Al. Lotników 32/46, PL-02-668 Warsaw, Poland

H. Wabnitz, S. Toleikis, K. Tiedtke

HASYLAB/DESY, Notkestr. 85 D-22607 Hamburg, Germany

M.Störmer

GKSS-Forschungszentrum Geesthacht GmbH, Max-Planck-Strasse 1 21502 Geesthach, Germany

A.J. Gleeson

CCRLC Daresbury Laboratory, Warrington, Cheshire, WA4 4AD, UK

Abstract:

We present results of damage studies conducted at the Free Electron LASer in Hamburg (FLASH) facility with 13.5 nm (91.8 eV) and 7 nm (177.1 eV) radiations. The laser beam was focused on a sample of 890 nm thick amorphous carbon coated on a silicon wafer mimicking a x-ray mirror. The fluence threshold for graphitization was determined for different grazing angles above and below the critical angle. The

observed angular dependence of F_{th} is explained by the variation in absorption depth and reflectivity. Moreover the absorbed local dose needed for the phase transition leading to graphitization is shown to vary with the radiation wavelength.

Introduction

Electron accelerator based x-ray Free-Electron Laser (FEL) light sources will deliver femtosecond milli-Joule light pulses in the keV photon energy range. The interaction of such light pulses with solids is not yet extensively investigated. This lack of knowledge represents a severe limitation for the design of the x-ray FEL optics. In fact, the FEL beam transport and the requirements of proposed experiments create highly demanding constraints on the x-ray optic elements. In addition to high performance all optical properties require stable operation under irradiation. It is hence of fundamental importance to understand the interaction mechanisms occurring at the surface of the optical elements.

A first step toward this understanding is to study the interaction of intense radiation using soft x-ray (XUV) FEL sources. Such studies have already been reported for 32.5 nm at normal incidence [1]. The present work extends these investigations in terms of wavelengths (down to 7 nm corresponding to 177.1 eV photon energy) and down to 4.3° grazing angle. We present results for amorphous Carbon (a-C) which is already in use at XUV FEL beamlines [2,3] and is a possible candidate for x-ray optics at the future hard x-ray FEL beamlines. The usual x-ray mirrors work in total external reflection geometry, i.e. the grazing angle is smaller than the critical angle θ_c defined for each wavelength as $\theta_c = \sqrt{(2\delta)}$ [4] where δ is the real part of the refractive index $n=1-\delta+i\beta$. In total external reflection geometry and the case of XUV radiation (i.e. a domain where δ is positive and β is non zero for materials) the electric field is propagating in the medium along the surface and decays with exponential dependence on depth [4]. The exponential decay corresponds to an absorption depth, distance normal to the surface, of few nanometres. The damage mechanism in this specific configuration should show differences compare to the normal incidence case. We are reporting of experimental investigations for different angles and wavelengths of the surface damage, defined as any irreversible modification of the optical properties of the initial material, below the ablation threshold.

Experiment

The experiment was performed at FLASH, the set-up has already been described in the reference [1]. The samples were placed in the focus of a 2 m focal length ellipsoidal mirror of the BL2 beamline [3]. A fast shutter enables to select a single pulse for which the energy is measured using a gas ionisation detector. The detector is located before the optical elements of the beamline, for which the total transmission has been measured to be 0.64 [3] at 13.5 nm, the same value is assumed at 7 nm. The grazing angle was determined with the following procedure: a CCD camera was mounted behind the sample holder in order to measure the direct beam position. Then the sample was inserted in the beam and the position of the reflected beam measured on the CCD camera. The distance sample to CCD, noted *a*, and the measured horizontal shift between the straight and the reflected beam, noted *b*, give the grazing angle $2.\alpha = \mathrm{atan}\,(b/a)$, with an accuracy of 0.2°. At 13.5 nm the grazing angles 18.7°, 15.1° and 4.3° were investigated and 10°, 7.7° and 4.3° at 7 nm, the critical angle θ_c being 15.8° for 13.5 nm and 8° for 7 nm. For each sample and each angle at least 60 single shots were recorded.

The samples consist of 890 nm thick a-C coating produced by magnetron sputtering on a Si wafer. This thickness was chosen to be larger than the attenuation depth at normal incidence in order to minimize the possible influence of the substrate. The coating was done at GKSS chamber using identical procedure than for the mirrors installed at the FLASH beamlines. The mean roughness was measured to be 0.4 nm. The sp^3/sp^2 ratio is a fundamental parameter of the material which has been shown to be directly proportional to the density [5]. From x-ray reflectivity measurement[6] we determined the density to be 2.2 g/cm³, leading to a sp^3 fraction of nearly 20 %.

Results.

The samples were investigated using Nomarski (differential interference contrast - DIC) microscope (see figure 1). Two concentric circles can be distinguished induced by two different damage processes corresponding to material expansion (outer part) and ablation (inner part). The most external circle corresponds to the lowest damage threshold. Selected spots were also investigated using atomic force microscopy confirming that this damage is a volume expansion. In the following we will focus on this first process which induces degradation of optical properties, therefore being of interest for x-ray FEL optics. The possible process for volume expansion, and therefore damage, is graphitization of a-C, i.e. phase transition from sp^3 to sp^2 bonding. This damage phenomenon is quite general for diamond-like material submitted to intense flux of photons[1,7] or particles. In the case of a-C, the exact structure of the final graphitized material can differ due to the large variety of possible carbon structures (graphite plane, nano-crystallite, rings[8]). Nevertheless, investigations of this aspect are underway but beyond the scope of the present letter.

For each spot the area of the outer contour was measured and correlated to the measured laser pulse energy. The dependence of the damaged surface to energy can then be plotted, as shown in figure 2 for the normal incidence case at both wavelengths, and the damage threshold energy E_{th} can be determined. In the case of 13.5 nm radiation the beam has nearly a Gaussian shape and data points were fitted (see figure 2) with a logarithmic function [9] allowing to determine E_{th}. In order to retrieve the fluence threshold F_{th} one needs to determine the beam radius. In the 13.5 nm case the radius was measured to be 5 µm (1/e radius), using a well established technique[10]. In the 7 nm case, the beam shows shape irregularities and prevents to use the Liu methods for determining E_{th}. Data points were then linearly fitted [see figure 2]. The beam diameter was determined using the Q-factor method [11] which allows retrieving a generalized area in the case of non-Gaussian beam. The focused beam spot area was found to correspond to a circle of 4.5 µm radius. This procedure is nevertheless less accurate explaining the larger uncertainty on F_{th}.

In figure 3 the resulting F_{th} as a function of the grazing angle are given. The values for 13,5 nm (7nm) are 171±40 mJ.cm^{-2} (195±46 mJ.cm^{-2}) in the normal incidence case, 47±7 mJ.cm^{-2} (35±11 mJ.cm^{-2}) at 18.75° (10°), 26±4 mJ.cm^{-2} (19±23 mJ.cm^{-2}) for 15.1° (7.7°) and 77±8 mJ.cm^{-2} (52±30 mJ.cm^{-2}) at 4.3°. The curves plotted in the figure 3 represent the ratio d_a / (1-R), d_a being the absorption depth and R the reflectivity[12]. This ratio directly relates the energy density effectively deposited in the material to F_{th}. The trends are very similar to the ones that can be inferred from the measurements and allows explaining the measured data in a very simple manner. In fact from normal incidence to the critical angle the absorption depth is decreasing (from 160 to 10 nm for 13,5 nm and from 632 to 12 nm for 7 nm) while the reflectivity stays very weak below 0.1. Hence the energy density increases inducing a decrease of F_{th}. Below θ_c the absorption length stays almost constant as the process of external total reflection occurs. In this case the radiation penetrates in the material on a nearly constant d_a value for angles smaller than θ_c (down to 4 nm for both wavelengths). At the same time the reflectivity is increasing up to 0.9 for both wavelengths at 4.3°, hence diminishing the energy really absorbed in the material. As a consequence the density of energy decreases and F_{th} is increasing as shown by the measured point.

In order to get a deeper insight in the physics of the interaction we calculated the absorbed dose per atom defined as $D_{th}= E_{th}\ (1-R) / (S.d_a.n_a)$, $n_a= 1.1\times10^{23}$ cm^{-3} being the atom density and S the focal spot area. Figure 4 presents the calculated dose as a function of the absorption depth. For both wavelengths the trend is similar: the dose increases for 13.5 nm (7nm) from 0.60±0.04 (0.13±0.05) to 0.89±0.13 (0.27±0.08), 1.00±0.16 (0.33±0.27) and finally 1.09±0.12 (0.69±0.40) eV/atom. There is a clear increase of D_{th} as d_a is decreasing, meaning that more energy is needed to damage the sample. We interpret this result as an effect of the electrons transport. In fact in the case of 4.3° grazing angle d_a is nearly 4 nm for both wavelengths and the inelastic mean free path in a-C [13] is in the order of 0.5 to 1 nm. Before recombining in the valence band, electrons will undergo several collisions and diffuse on a depth larger than d_a. Therefore a fraction of the energy is carried away from the effectively irradiated volume by the electrons. This process lowers the amount of energy available for the damage process explaining the observed increase of D_{th}.

Furthermore figure 2 also shows that D_{th} depends on the wavelength: 7 nm values being lower than for the 13.5 nm case. Theoretical studies[14,15] for optical wavelengths have shown that a non-equilibrium distribution of electron excited by a femtosecond laser pulse results in lowering of the energy barrier between diamond and graphite structure. As a consequence the higher the electron temperature (T_e), the lower the energy barrier is. The 7 nm radiation should excite a distribution of electrons having a higher T_e than 13,5 nm, as in both case the same valence band electrons are ionized. Therefore the transient energy barrier energy is lower in the 7 nm case which also lowers the value of D_{th} needed for the phase transition. The wavelength dependence can then be explained, in the framework of this model, by the non-thermal origin of the damage observed.

Conclusion

To summarize we have measured the fluence damage threshold for a-C at two different wavelengths for grazing angles above and below the critical angle. The present study demonstrates the effects electron transport and the non-thermal origin of the damage process which induces a dependence on the wavelength. If one now considers the hard x-rays range, i.e. photon energy in the keV range, the effect of electron transport should become more efficient as the inelastic mean free path increase with higher kinetic energy. On the other hand, in the specific case of carbon as the electronic temperature should also increase, the threshold dose for damage should also decrease. Our results also emphasize that considering thermal melting as a threshold for damage, defined as irreversible modification of the optical properties, is at least for carbon not a safe criteria for the design of the beamline.

Acknowledgment:

The authors greatly thank the support of the FLASH scientific and technical team for their help during the beamtime enabling a successful experiment. Financial support from Czech Ministry of Education (projects LC510, LC528, and LA08024), Academy of Sciences of the Czech Republic (projects KAN300100702, Z10100523, IAAX00100903, and IAA400100701), and Grant Agency of the Czech Republic (202/08/H057) is greatly appreciated.

[1] S.P. Hau-Riege, R.A. London, R.M. Bionta, M.A. McKernan, S.L. Baker, J. Krzywinsky, R. Sobierajski, R. Nietubyc, J.B. Pelka, M. Jurek, L. Juha, J Chalupský, J. Cihelka, V. Hájková, A. Velyhan, J. Krása, J. Kuba, K. Tiedtke, S. Toleikis, Th. Tschentscher, H. Wabnitz, M. Bergh, C. Caleman, K. Sokolowski-Tinten, N. Stojanovic and U. Zastrau. Appl. Phys. Lett. **90**, 173128 (2007)

[2] B. Steeg, L. Juha, J. Feldhaus, S. Jacobi, R. Sobierajski, C. Michaelsen, A. Andrejczuk and J. Krzywinski, Appl. Phys. Lett. **84**, 657 (2004)

[3] K. Tiedtke, A. Azima, N. von Bargen, L. Bittner, S. Bonfigt, S. Düsterer, B. Faatz, U. Frühling, M. Gensch, Ch. Gerth, N. Guerassimova, U. Hahn, T Hans, M Hesse, K Honkavaar1, U. Jastrow, P. Juranic, S. Kapitzki, B. Keitel, T. Kracht, M. Kuhlmann, W. B. Li, M. Martins, T. Núñez, E. Plönjes, H. Redlin, E. L. Saldin, E. A. Schneidmiller, J. R. Schneider, S. Schreiber, N. Stojanovic, F. Tavella, S. Toleikis, R. Treusch, H. Weigelt, M. Wellhöfer, H. Wabnitz, M. V. Yurkov and J Feldhaus, New J. Phys. **11**, 023029 (2009)

[4] D. Attwood, “Soft x-ray and extreme ultraviolet radiation” Cambridge University Press, 1999

[5] J. Robertson, Mater. Sci. Eng. **R37**, 129 (2002)

[6] M. Störmer, C. Horstmann, D. Häussler, E. Spiecker, F. Siewert, F. Scholze, F. Hertlein, W. Jäger and R. Bormann, SPIE Proc. **70077**, 707705 (2008)

[7] G. Dumitru, V. Romano, H.P. Pimenov, T. Kononenko, M. Sentis, J. Hermann, S. Bruneau, Appl. Surf. Sci. **222**, 226 (2004)

[8] A.C. Ferrari and J. Robertson, Phys. Rev. B **61,** 14095 (2000)

[9] J.M. Liu, Opt. Lett. **7**,196 (1982)

[10] J. Chalupsky, L. Juha, J. Kuba, J. Cihelka, V. Háková, S. Koptyaev, J. Krása, A. Velyhan, M. Bergh, C. Caleman, J. Hajdu, R. M. Bionta, H. Chapman, S. P. Hau-Riege, R. A. London, M. Jurek, J. Krzywinski, R. Nietubyc, J. B. Pelka, R. Sobierajski,

J. Meyer-ter-Vehn, A. Krenz-Tronnier, K. Sokolowski-Tinten, N. Stojanovic, K. Tiedtke, S. Toleikis, T. Tschentscher, H. Wabnitz, and U. Zastrau, Opt. Expr. **15**, 6036 (2007)

[11] J. Chalupsky, J. Krzywinski, L. Juha, V. Hájková, J. Cihelka, T. Burian, L. Vyšín, J. Gaudin, A. Gleeson, M. Jurek, A. R. Khorsand, D. Klinger, H. Wabnitz, R. Sobierajski, M. Störmer, K. Tiedtke, and S. Toleikis, "Spot size characterization of focused non-Gaussian beams", *to be submitted.*

[12] Centre for X-Ray Optics: http://henke.lbl.gov/optical_constants/

[13] B. Ziaja, D. van de Spoel, A. Szöke and J. Hadju, Phys. Rev. B **64**, 214104 (2001)

[14] C.Z. Wang, K.M. Ho, M.D. Shirk, and P.A. Molian, Phys. Rev. Lett. **85**, 4092 (2000)

[15] H.O. Jeschke, M.E. Garcia and K.H. Bennemann, Phys. Rev. B **60**, R3701 (1999)

Figure caption:

Figure 1 : Nomarski microscope images of damage by 13,5 nm beam at normal incidence (left) and 18,5° grazing angle (right). The scale is the same for both images.

Figur 2: Diameter of damage corresponding to graphitization as a function of the impinging laser pulse energy. Both curves correspond to the normal incidence case. The curves represent fits used to determine E_{th}.

Figure 3: Threshold fluence for damage as a function of grazing angle. The curves show the ratio $d_a/(1-R)$, normalised with a constant in order to scale the experimental data. The value of Θ_c are indicated on the top for both wavelengths.

Figure 4: Absorbed dose as a function of absorption depth.

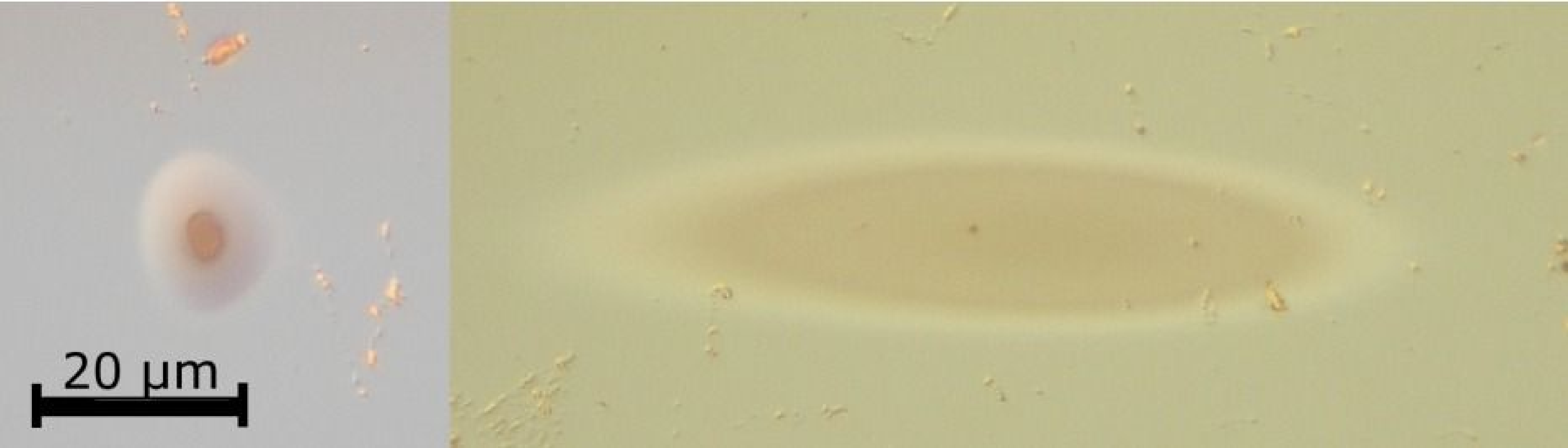
20 µm

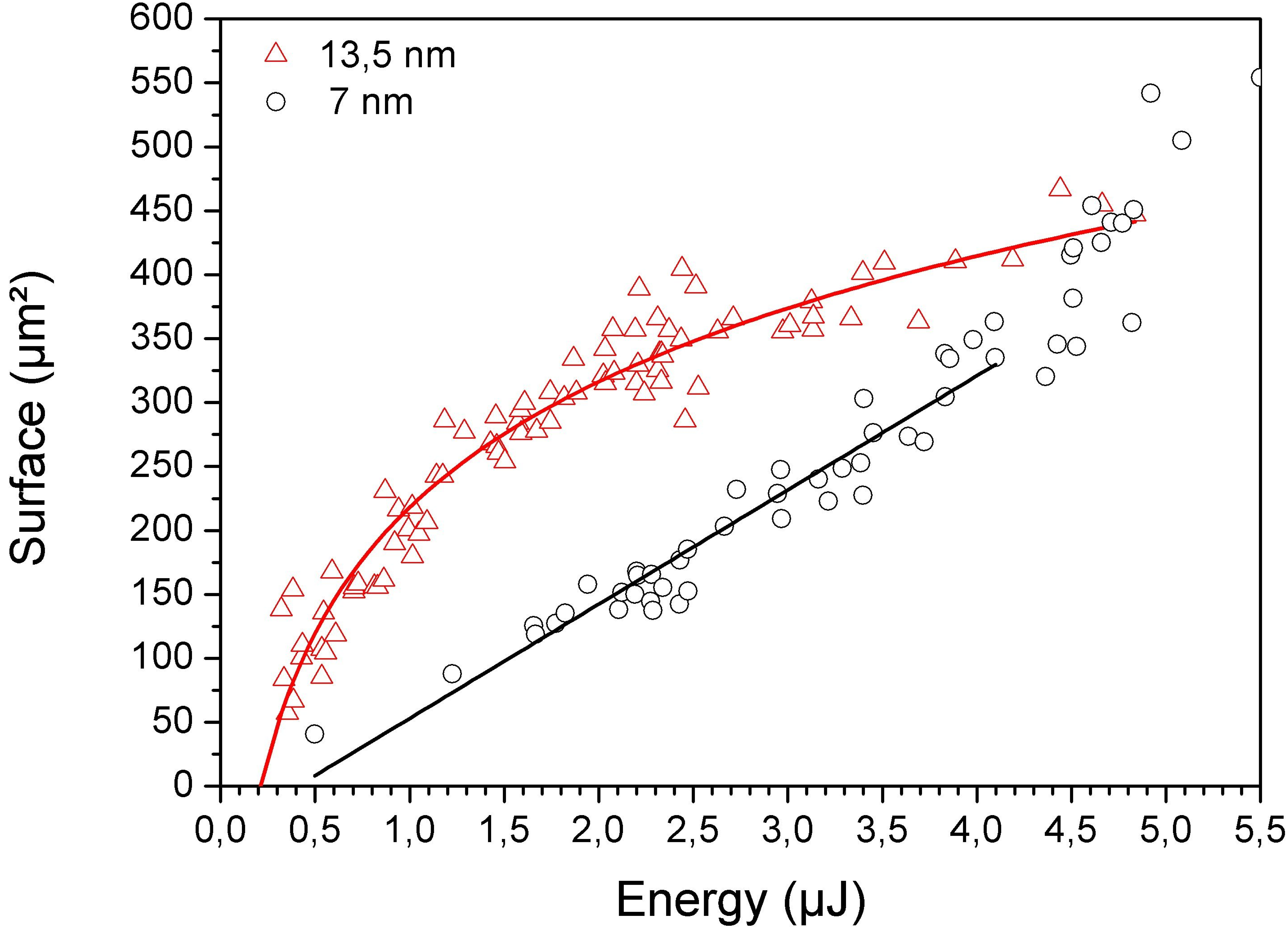

600
550
500
450
400
350
300
250
200
150
100
50
0
Surface (µm²)
0,0
0,5
1,0
1,5
2,0
2,5
3,0
3,5
4,0
4,5
5,0
5,5
Energy (µJ)
13,5 nm
7 nm

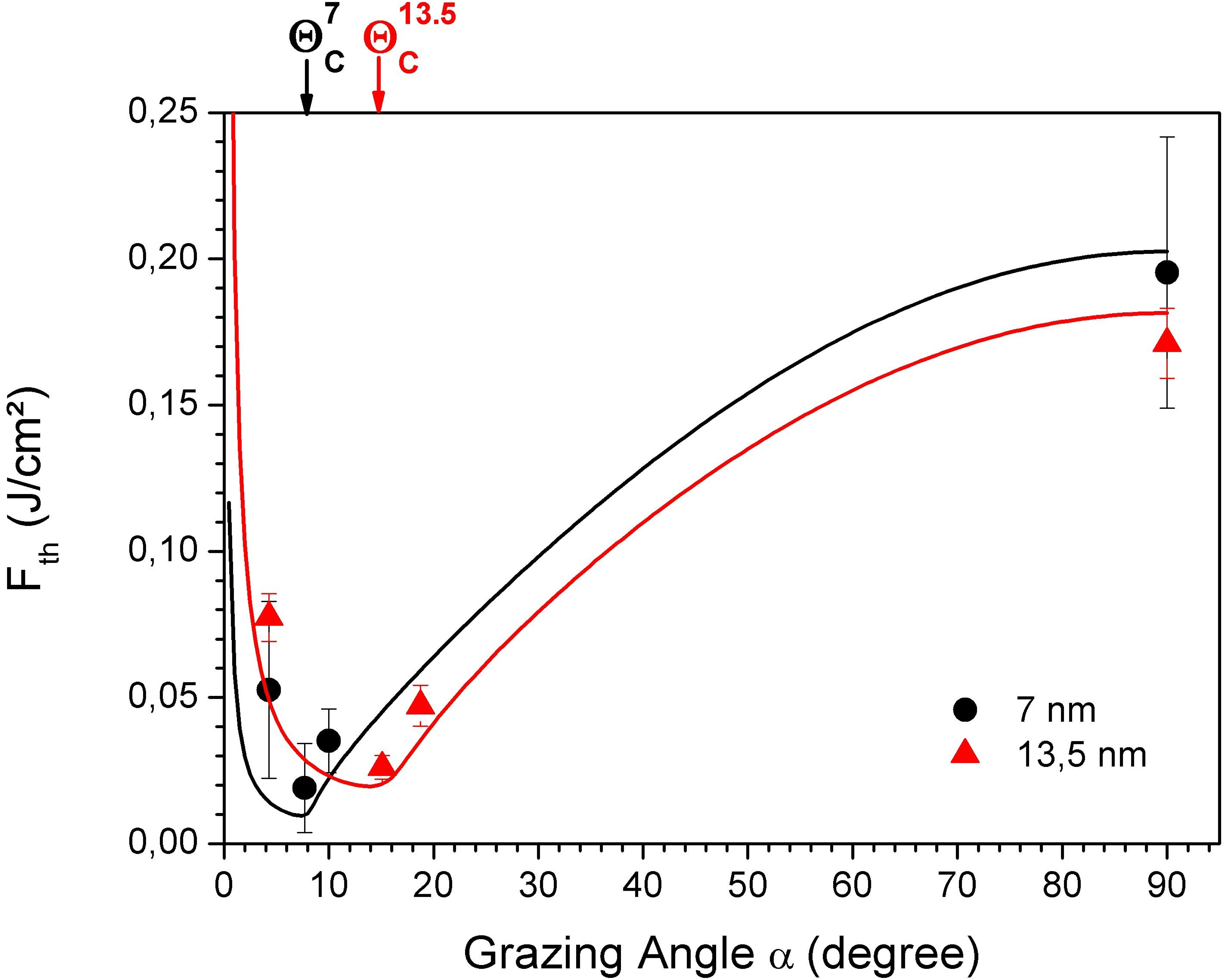

Θ_C^7
Θ_C^13.5
0,25
0,20
0,15
0,10
0,05
0,00
F_th (J/cm²)
0
10
20
30
40
50
60
70
80
90
Grazing Angle α (degree)
7 nm
13,5 nm

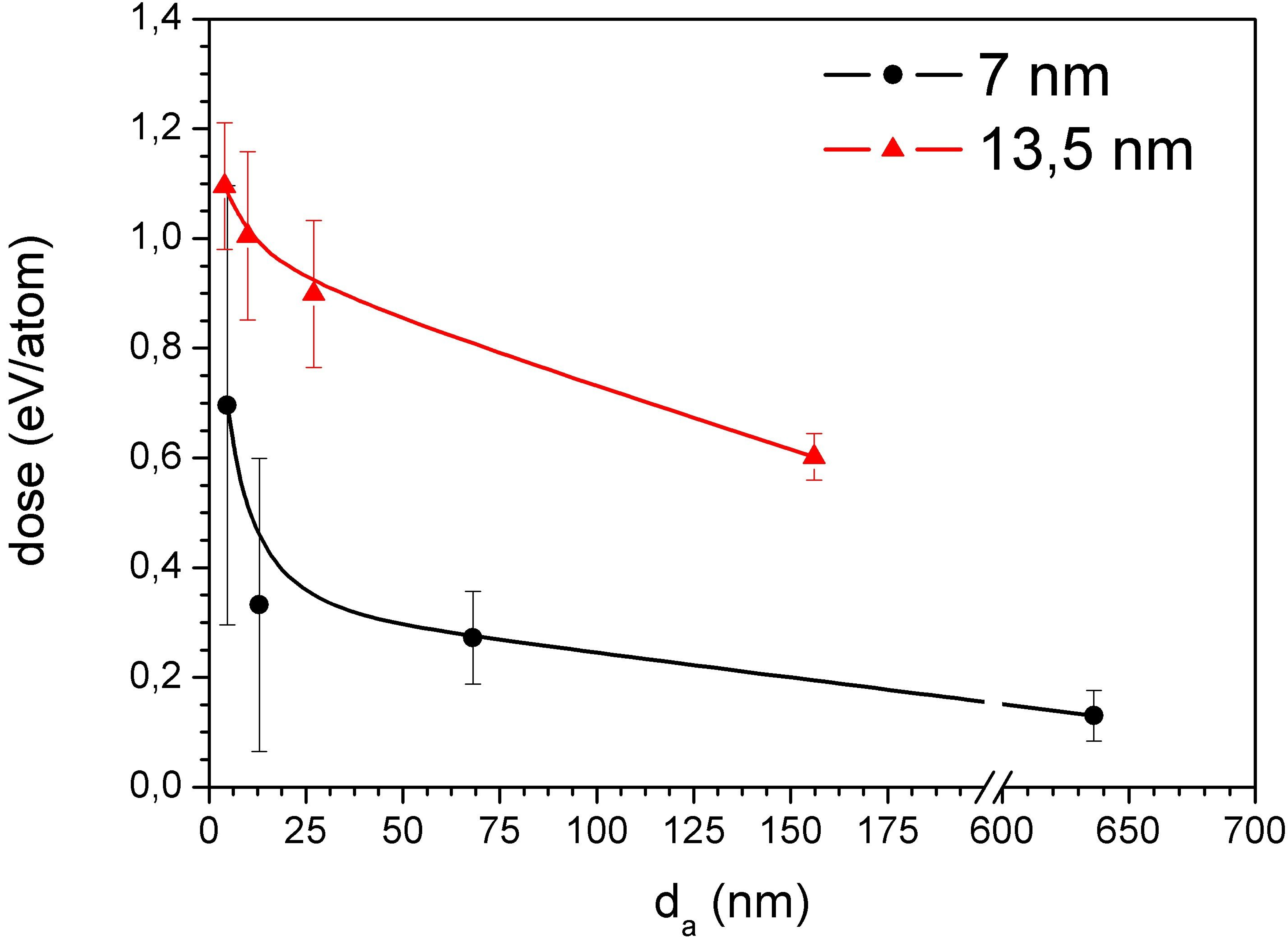

dose (eV/atom)
1,4
1,2
1,0
0,8
0,6
0,4
0,2
0,0
0
25
50
75
100
125
150
175
600
650
700
d$_a$ (nm)
7 nm
13,5 nm